OXFORD GENETICS

GENETICS, 2022, 220(1), iyab170
https://doi.org/10.1093/genetics/iyab170
Advance Access Publication Date: 11 October 2021
Investigation
Highlighted Article

The entomopathogenic nematode *Steinernema hermaphroditum* is a self-fertilizing hermaphrodite and a genetically tractable system for the study of parasitic and mutualistic symbiosis

Mengyi Cao ,*† Hillel T. Schwartz ,† Chieh-Hsiang Tan ,† and Paul W. Sternberg *

Division of Biology and Biological Engineering, California Institute of Technology, Pasadena, CA 91125, USA

*Corresponding author: pws@caltech.edu (P.W.S.); mengcao@caltech.edu (M.C.)
†These authors contributed equally to this work.

Abstract

Entomopathogenic nematodes (EPNs), including *Heterorhabditis* and *Steinernema*, are parasitic to insects and contain mutualistically symbiotic bacteria in their intestines (*Photorhabdus* and *Xenorhabdus*, respectively) and therefore offer opportunities to study both mutualistic and parasitic symbiosis. The establishment of genetic tools in EPNs has been impeded by limited genetic tractability, inconsistent growth *in vitro*, variable cryopreservation, and low mating efficiency. We obtained the recently described *Steinernema hermaphroditum* strain CS34 and optimized its *in vitro* growth, with a rapid generation time on a lawn of its native symbiotic bacteria *Xenorhabdus griffiniae*. We developed a simple and efficient cryopreservation method. Previously, *S. hermaphroditum* isolated from insect hosts was described as producing hermaphrodites in the first generation. We discovered that CS34, when grown *in vitro*, produced consecutive generations of autonomously reproducing hermaphrodites accompanied by rare males. We performed mutagenesis screens in *S. hermaphroditum* that produced mutant lines with visible and heritable phenotypes. Genetic analysis of the mutants demonstrated that this species reproduces by self-fertilization rather than parthenogenesis and that its sex is determined chromosomally. Genetic mapping has thus far identified markers on the X chromosome and three of four autosomes. We report that *S. hermaphroditum* CS34 is the first consistently hermaphroditic EPN and is suitable for genetic model development to study naturally occurring mutualistic symbiosis and insect parasitism.

Keywords: symbiosis; mutualism; parasitism; entomopathogenic; nematode; hermaphroditism; Steinernema; Xenorhabdus; model system; genetic screen

Introduction

Microbial symbiosis ranges across a wide spectrum from mutualistic (beneficial) interactions to parasitism (Figure 1A). Mutualistic and parasitic relationships are ubiquitous on earth in all animals and have important effects on metabolism, immune response, development, and behavior, ultimately impacting the health and shaping the evolution of host animals (Ruby 2008; McFall-Ngai *et al.* 2013; Morais *et al.* 2021). Currently, studies of the genetic basis for multicellular partners engaging in mutualistic interactions are mostly restricted to traditional model organisms with simplified consortia or synthetic microbiomes, such as hydra, fruit fly, zebrafish, mice, and more recently microbiome studies of the free-living soil nematode *Caenorhabditis elegans* (Bosch *et al.* 2019). Genetic tools have not existed with which to systematically study the animal host side of any naturally occurring interactions with their mutualistic microbes, especially in a binary and species-specific manner.

Caenorhabditis elegans has been a highly productive laboratory organism for investigating the genetic bases underlying a broad range of biological questions including how genes specify complex structures and behaviors (Brenner 1974). An equally tractable nematode system with a naturally occurring species-specific microbial symbiosis could be similarly productive in studying symbiotic interactions. The reproductive mode of *C. elegans* consists of self-fertilizing hermaphrodites and males, greatly facilitating genetic screens that use mutagenesis to rapidly produce a large number of mutants (Brenner 1974). These mutants provided genetic markers to establish the basic genetic features of the organism and led to the discovery of novel phenotypes and important biological mechanisms (Brenner 1974; Horvitz 2003; Fire 2007; Mello 2007). Large collections of publicly available mutants and rich genetic tools in the wild-type isolate N2 and diverse natural isolates of *C. elegans* have more recently facilitated the study of the genetics of host animals including their interactions with intestinal microbiomes and bacterial pathogens they encounter in the wild (Frézal and Félix 2015; Shapira 2017; Kim and Flavell 2020; Zhang *et al.* 2021). However, *C. elegans* lacks a stable and species-specific mutualistic

Received: August 25, 2021. **Accepted:** September 29, 2021

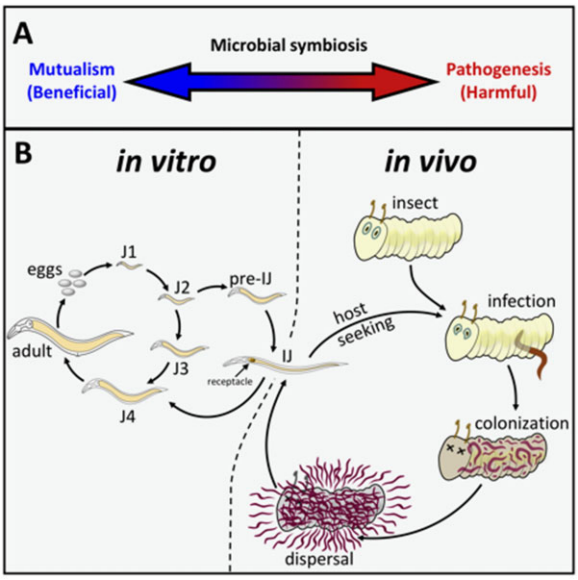

Figure 1 Mutualistic and parasitic life cycle of *S. hermaphroditum*. (A) The relationship between a microbe and its animal host can be considered to be on a continuum between mutualism, from which both organisms benefit, and pathogenesis, in which one species is entirely harmful to the other. (B) The life cycle of the EPN *S. hermaphroditum*. The reproductive development of *S. hermaphroditum* can be monitored during growth *in vitro*, on Petri plates: the worm passes through four larval stages, J1–J4; then becomes an adult, which produces fertilized embryos in eggs that can be laid or can hatch internally, to begin the cycle again. The second larval stage can alternatively develop into a developmentally arrested, stress-resistant IJ, analogous to the dauer stage of *C. elegans*. The IJ has a specialized receptacle in its anterior intestine containing viable cells of its bacterial symbiont *X. griffiniae*. The IJ will seek out an insect host, invade its body, and resume development, reentering the reproductive life cycle. As it exits developmental arrest the worm will release its bacterial cargo. Together the worm and its bacteria kill the insect, and the bacteria convert the carcass into a nutritive food source for the worm and for generations of its progeny. When the food source is exhausted a new generation of worms will develop as IJs and will seek out new hosts.

symbiont and is free-living rather than a parasite, and so cannot be used to investigate the complete range of symbiotic interactions.

Following the establishment of *C. elegans* as a genetic model system, genetic tools have been developed in other nematode species to study their molecular ecology, evolution, and multi-organism interactions, including predator–prey, necromenic, and parasitic relationships (Kroetz *et al.* 2012; Lightfoot *et al.* 2019; Gang *et al.* 2020; Liu *et al.* 2020). However, the limited number and diversity of nematode species that have been developed for genetic research does not match the potential that nematodes have to increase our understanding of diverse biological fields, including symbiotic and parasitic interactions. For instance, although parasitic nematodes infect all animal species and cause major medical problems, the characterization of molecular mechanisms in nematode infections is restricted to a few species of human parasite due to limitations of genetic tools, ethical concerns, and difficulties of culturing parasitic nematodes *in vitro* (Lok 2019). Despite the limitations imposed by its free-living, non-parasitic lifestyle in the wild, *C. elegans* is still the major genetic model nematode for most molecular ecology studies. Establishing genetic systems in parasitic nematodes that are culturable and tractable in the laboratory will greatly expand our knowledge of parasitism and help to identify conserved molecular pathways in the process of infection, such as host-seeking behaviors and parasite-derived immunomodulatory effectors (Gang and Hallem 2016; Bobardt *et al.* 2020).

Heterorhabditis and *Steinernema* entomopathogenic nematodes (EPNs) each have a species-specific association with mutualistic bacteria (*Photorhabdus* and *Xenorhabdus*, respectively; Figure 1; Forst and Clarke 2002; Goodrich-Blair and Clarke 2007). The symbiotic pairs are used commercially in agriculture as an organic pest control mechanism (Ehlers 2001; Tarasco *et al.* 2017). When food source is limited and nematode population is dense, EPNs can become developmentally arrested, stress-resistant infective juvenile (IJ) analogous to the dauers of free-living nematodes. IJs carry symbiotic bacteria in their intestine as they seek their insect prey. IJs invade an insect and exit from developmental arrest, molting into the fourth juvenile stage (J4) while releasing their symbiotic bacteria into the insect (Ciche and Ensign 2003; Snyder *et al.* 2007). When delivered internally even a very small number of *Xenorhabdus* and *Photorhabdus* bacteria, on the order of <5 colony-forming units (CFUs), can rapidly kill an insect and reproduce in its cadaver, providing a rich food source for their nematode partner, while inhibiting other microbes and animals from consuming the cadaver (Goodrich-Blair and Clarke 2007). EPN reproductive development includes four stages of juveniles (J1–J4, analogous to the four larval stages L1–L4 of *C. elegans*). Exhaustion of the bacterially colonized insect cadaver as a food source signals the nematodes to cease reproductive development and instead produce IJs after the first juvenile stage (developing from J2 to pre-IJ to IJ; similar to the development of *C. elegans* from L1 to L2d to dauer) and disperse from the insect cadaver seeking new insect hosts (Forst and Clarke 2002).

The ability to culture EPNs in the laboratory and the availability of genetic manipulation of symbiotic bacteria would make them valuable systems to study fundamental principles of microbial symbiosis ranging from mutualism to parasitism. This includes bacteria-nematode recognition and nutritional codependence, nematode toxin secretion, host-seeking behaviors, and comparative genomics (Herbert and Goodrich-Blair 2007; Hallem *et al.* 2011; Dillman *et al.* 2012, 2015; Chaston *et al.* 2013; Chang *et al.* 2019). However, no stable genetic tools or comprehensive genetic system has been established in any EPN species despite efforts from multiple groups over decades (Hashmi *et al.* 1995; Ciche and Sternberg 2007; Ratnappan *et al.* 2016). The lack of efficient cryopreservation methods in EPNs has led to potential issues of inbreeding depression in laboratory strains (Hopper *et al.* 2003). In addition, most of the currently available nematode genetic models took advantage of consistent hermaphroditism similar to *C. elegans*, greatly facilitating screens for homozygous F_2 progeny of mutagenized animals produced by self-reproduction and the maintenance of mutant lines that might be incapable of mating (Brenner 1974; Sommer 2006; Shinya *et al.* 2014). Both *Heterorhabditis* and *Steinernema* lack consistently hermaphroditic species, which has impeded development of forward genetic tools. *Heterorhabditis* alternates between hermaphrodite and female in insects, and when grown on Petri plates produces almost exclusively females after the first generation that recovers from IJ as hermaphrodites, with a low percentage of males that diminishes in successive generations (Dix *et al.* 1992; HTS and PWS, unpublished). Existing strains of *Steinernema* have been strictly male–female (gonochoristic). The only exception is *S. hermaphroditum*-Indonesia, described as producing one generation of hermaphrodites (Griffin *et al.* 2001; Stock *et al.* 2004). However this isolate was subsequently lost. To date, forward genetics screens in *Heterorhabditis* have produced only a few mutants, insufficient

to establish the species as a genetic model (Cohen-Nissan *et al.* 1992; Rahimi *et al.* 1993; HTS and PWS, unpublished), and no attempts to perform forward genetic screens in *Steinernema* have been reported.

In this research, we obtained a recently described isolate of *S. hermphroditum*, the Indian strain CS34 (Bhat *et al.* 2019), and developed protocols for continuous cultivation *in vitro* on agar media in Petri plates. *Steinernema hermaphroditum* can be grown on various bacterial species, including its native symbiont. *In vitro* growth led us to discover that CS34 is consistently hermaphroditic, with healthy autonomously reproducing hermaphrodites and spontaneous functional males. We stabilized the genetic background of the wild isolate by repeated inbreeding for a controlled number of generations and established efficient cryopreservation to facilitate maintenance of the wild type and collections of mutant strains. We performed ethyl methane sulfonate (EMS) mutagenesis screens and isolated multiple recessive mutants with classical phenotypes such as dumpy (Dpy) and uncoordinated (Unc). Mutant hermaphrodites were mated with wild-type males and heterozygous F_1 animals produced F_2 progeny that showed segregation according to Mendelian ratios, proof that these animals reproduce by self-fertilization rather than parthenogenesis. 4′,6-diamidino-2-phenylindole (DAPI) staining of oocytes of hermaphrodites revealed five pairs of chromosomes. Our initial mapping efforts assigned some of the current mutant alleles into at least four of the five linkage groups, including an X chromosome that determines the sex of this species. Here, we report the first consistently hermaphroditic EPN, the *S. hermaphroditum* isolate CS34, and demonstrate that it is convenient to culture and cryopreserve in the laboratory and is highly genetically tractable. We propose that this species has great potential to further expand our understanding of the genetic bases of a variety of molecular signaling pathways, especially in microbial symbiosis.

Materials and methods

Nematode maintenance and bacterial culture

Conventional (in contrast to germ-free or axenic) IJs are defined as those colonized by their bacterial symbiont. Conventional IJs of *S. hermaphroditum* were propagated through infection of fifth-instar larvae of the wax moth *Galleria mellonella* (PetSmart, Phoenix, AZ) and recovered using a modified White trap (White 1927). IJs were trapped in distilled water and maintained in 15 ml culture flasks (Corning, Corning, NY). To culture *S. hermaphroditum in vitro*, nematodes were grown on bacterial lawns on the surface of agar media in Petri plates. To grow symbiotic bacterial lawns, individual colonies of *X. griffiniae* were picked from Luria Bertani agar supplemented with 0.1% sodium pyruvate (LB-pyruvate; Xu and Hurlbert 1990) and used for inoculating liquid media. Cultures were grown in LB broth kept in the dark (dark LB) overnight at 30°C with shaking or in 2% proteose peptone No. 3 with 0.1% sodium pyruvate overnight at room temperature without shaking. Bacterial cultures were seeded onto lipid agar media (per liter: 15 g bacto agar, 8 g nutrient broth, 5 g yeast extract, 2 g $McCl_2{\cdot}6H_2O$, 1 g sodium pyruvate, 7 ml corn syrup, and 4 ml corn oil; Vivas and Goodrich-Blair 2001) or nematode growth media (NGM) agar (Brenner 1974) supplemented with 0.1% by volume of 5 mg/ml cholesterol in ethanol.

Symbiotic bacteria isolation and nematode growth

Steinernema hermaphroditum IJs were concentrated by centrifugation, surface-sterilized by treatment with 1% bleach for 2 min with gentle shaking, concentrated by centrifugation, and washed in distilled water three times. Approximately 200 IJs were resuspended in 200 µl dark LB media and ground for two minutes using a hand homogenizer (Kimble Pellet Pestle Cordless Motor, DWK Life Sciences, Millville, NJ). Samples were examined using microscopy to confirm that grinding of IJs was complete. Homogenate was serially diluted to 1:10, 1:100, 1:1000, and 1:10,000 in dark LB. Each dilution was plated on LB-pyruvate agar and incubated at 30°C overnight. Dilutions that produced 10–100 colonies were counted to estimate CFUs per IJ. Ten individual colonies were purified by restreaking onto LB-pyruvate agar followed by isolating single colonies. Symbiotic bacterial isolates were frozen at −80°C after mixing 900 µl of overnight bacterial culture with 600 µl of LB-glycerol (50% LB, 50% glycerol). One *X. griffiniae* isolate was given the name HGB2511 (Supplementary Table S1) and was used as the principal food source for culturing *S. hermaphroditum* on agar media.

16S rRNA gene sequence determination from symbiotic bacterial isolates

To extract genomic DNA, overnight cultures of symbiotic bacteria were pelleted by centrifugation at maximum speed in a table top microcentrifuge (~16,000 rcf) for 1 min. The bacterial pellet was resuspended in 50 µl distilled water, boiled at 100°C for 10 min, incubated on ice for 10 min, and centrifuged at maximum speed in a microcentrifuge to remove debris. Supernatant containing genomic DNA was used as a template for the PCR amplification of the 16S rRNA gene using *Taq* polymerase (New England Biolabs, Ipswich, MA) and the primers oMC98f (5′-GAAGAGTTTGATCA TGGCTC-3′) and oMC99r (5′-AAGGAGGTGATCCAGCCGCA-3′) as previously described (Tailliez *et al.* 2006). An ~1500 bp PCR product was isolated using agarose gel electrophoresis and purified using QIAprep (QIAGEN, Valencia, CA). Sanger-sequencing was performed by Laragen (Culver City, CA) using primers oMC98f, oMC99r, oMC100r (5′-ACCGCGGCTGCTGGCACG-3′), and oMC101r (5′-CTCGTTGCGGGACTTAAC-3′). The 16S rRNA gene sequence was compared with existing rRNA gene sequences in the NCBI database using BlastN (NCBI Resource Coordinators 2017).

Growth rate analysis under different culture conditions

Embryos of *S. hermaphroditum* were obtained by treating gravid hermaphrodites with NaOH and NaOCl similar to methods used for *C. elegans* (Stiernagle 2006). The centrifugation process of embryo extraction was performed using a clinical centrifuge with a uniform speed. Briefly, gravid hermaphrodites cultured with *X. griffiniae* on NGM at 25°C were washed off the plates with M9 buffer (per liter: 3 g KH_2PO_4, 6 g Na_2HPO_4, 5 g NaCl, with 1 ml 1 M $MgSO_4$ added after autoclaving). The nematode suspension was then centrifuged to remove the supernatant, and water was added for a total volume of 3.5 ml. 0.5 ml of 5M NaOH and 1 ml of household bleach (8% available chlorine) were then added to the solution. The solution was mixed by gently shaking and allowed to react for 4–6 min, after which the embryos were collected by centrifugation. Embryos were then washed with 10 ml of M9 buffer three times, then centrifuged to remove the supernatant. Embryos were resuspended in M9 and seeded onto NGM agar Petri plates on which bacterial lawns had been grown. For growth rate analysis of worms fed with different bacteria, the bacterial strains used were *X. griffiniae* HGB2511, *Comamonas aquatica* DA1877, *Escherichia coli* OP50, and *E. coli* HB101 (Supplementary Table S1). Petri plates containing the bacterial lawns and embryos were cultured at 25°C. To assess the effects of temperature

on growth, embryos were placed on *X. griffiniae* HGB2511 bacterial lawns and incubated at 20°C, 25°C, 27.5°C, and 30 C. Nematodes on these plates were imaged every 12 h using WormLab equipment and software (MBF Bioscience, Williston, VT) until 120 h had elapsed unless the animals were first obscured by the growth of their progeny. Body length was measured by drawing a line from head to tail through the midline of each worm using ImageJ (NIH) software similarly to an established method (Roh *et al.* 2012).

Cryopreservation of *S. hermaphroditum*

Steinernema hermaphroditum cryopreservation was adapted from a trehalose-DMSO freezing protocol for *C. elegans* (O'Connell, 2021). Briefly, nematodes were grown on NGM agar seeded with *X. griffiniae* bacteria until the food was nearly exhausted. A mixed stage population of juvenile nematodes (mostly J1 nematodes that had hatched internally inside their hermaphrodite mothers) were washed off the agar in M9 buffer. Nematodes were concentrated by centrifugation for 1 min at ~1000 rcf and washed in 5 ml of trehalose-DMSO solution (per liter: 30.2 g trehalose, 35.4 ml DMSO, filter-sterilized), then incubated in 5 ml trehalose-DMSO solution for more than 30 min. Samples were transferred into cryotubes, placed in sealed Styrofoam boxes to slow their temperature change, and then placed in a −80°C freezer overnight before being transferred to cardboard boxes in a −80°C freezer.

Dissection and staining of the *S. hermaphroditum* gonad

A protocol for dissection and staining of the *S. hermaphroditum* gonad was adapted from gonad dissection and staining protocols developed for *C. elegans* (Kocsisova *et al.* 2018, 2019). Briefly, young adult hermaphrodites (1 day post-J4) were picked into a watchglass (Carolina Biological Supply Company, Burlington, NC) containing phosphate-buffered saline (PBS). Worms were washed three times on the watchglass with PBS and immobilized with levamisole (final concentration 200 μM). The worms were then dissected at the pharynx with a pair of 30G 5/8″ needles (PrecisionGlide, BD, Franklin Lakes, NJ). The dissected gonads were fixed with 3% paraformaldehyde (EM Grade, Electron Microscopy Science, Hatfield, PA) in PBS and postfixed with 100% methanol. Fixed gonads were then rehydrated and washed three times with PBSTw (PBS + 0.1% Tween-20). Following the washes, the gonads were incubated overnight at room temperature with a monoclonal anti-Major Sperm Protein (MSP) antibody (4A5, Developmental Studies Hybridoma Bank, University of Iowa; Kosinski *et al.* 2005)) diluted 1:10 in 30% goat serum (Thermo Fisher Scientific, Waltham, MA) in PBS. The gonads were then washed three times with PBSTw and incubated with secondary antibodies (Goat anti-Mouse Alexa Fluor 555; A-21424, Invitrogen) diluted 1:400 in 30% goat serum in PBS for 4 h at room temperature. Following the secondary staining, the gonads were again washed three times with PBSTw and resuspended in 1 drop of Vectashield containing DAPI (Vector Laboratories, Burlingame, CA). The gonad was finally mounted on pads of 5% agarose in water on microscope slides and covered with a cover glass (Sulston and Horvitz, 1977; Kocsisova *et al.* 2018). For gonads with only DAPI staining, antibody staining steps were skipped.

Image acquisition

Photomicrographs in Figures 2, B and C and 4 were acquired with a Zeiss Imager Z2 microscope equipped with Apotome 2 and Axiocam 506 mono using Zen 2 Blue software. Figure 3, A–D were acquired through the WormLab (MBF Bioscience, Williston, VT) equipment and software. The camera was a Nikon AF Micro 60/2.8D with zoom magnification.

EMS mutagenesis and screening for visible mutants

EMS mutagenesis of *S. hermaphroditum* was adapted from the standard protocol used for *C. elegans* (Brenner 1974). Unseeded and *X. griffiniae* seeded NGM agar were used throughout the EMS screen, and will be referred to as unseeded plates and bacterial lawns, respectively. Animals were hand-picked by developmental stage onto an unseeded plate, suspended in M9 buffer, and collected in a 15 ml conical tube. Nematodes were rinsed with M9 and incubated for 4 h at 20°C in 4 ml of M9 containing 20 μl EMS (46 mM), rotating on a cell culture wheel to avoid settling. Animals were pelleted by centrifugation (1 min, ~1000 rcf) and rinsed several times with M9, then allowed to recover for at least 30 min at room temperature on a bacterial lawn. After recovery, animals were transferred to new bacterial lawns with one to five animals per plate. Mutagenesis was performed using mid-J4 larvae, late-J4 larvae, and young adult hermaphrodites in our initial trials. Young adults were found to be the most productive stage to mutagenize.

The F_2 progeny of mutagenized animals were examined for possible mutant phenotypes (Figure 5A), either on the same plate the mutagenized animals had been growing on, or by transferring the progeny of the mutagenized animals to new plates to avoid exhausting the food source. When transferring, animals were either washed off the plate using M9 or moved within a chunk of agar cut by heat-sterilized metal spatula. Nematodes were then placed on the surface of another larger Petri plate (10 cm in diameter) containing NGM agar seeded with *X. griffiniae*. Mutants were tracked to identify the mutagenized P_0 animal or animals from which they descended, to avoid repeated recovery of animals with the same phenotype that might have arisen from the same mutagenesis event. Candidate mutants were picked to bacterial lawns and their self-progeny were examined for the propagation of a mutant phenotype. Stable mutant lines were mated with wild-type males to test for recessiveness and for linkage to the X chromosome.

To test for linkage between two mutations, we generated animals carrying both mutations as heterozygotes with wild-type alleles, in *trans* to each other if they were linked. Except in rare cases of mutants that could mate as homozygous or hemizygous males, this was done by first mating wild-type males to one of the two mutant strains. We then recovered F_1 males from the cross and mated them to the second mutant strain. Individual cross progeny from this second cross were placed on NGM agar Petri plates seeded with *X. griffiniae* and allowed to propagate. All of these animals would be heterozygous for the second mutation, but only half would carry the first mutation; these animals were identified by examining their progeny. From plates derived from animals heterozygous for both mutations we identified animals whose phenotype indicated they were likely to be homozygous for one of the two mutations present and placed each onto a bacterial lawn. By examining the progeny of these animals we first confirmed that they were homozygous for the mutation selected and then scored for animals phenotypic for the other mutation, which would mean their parent had one parental genotype and one recombinant genotype. Unlinked mutations would be expected to be present two-thirds of the time; tightly linked mutations should rarely be present. This approach was chosen because not all mutant phenotypes could be unambiguously

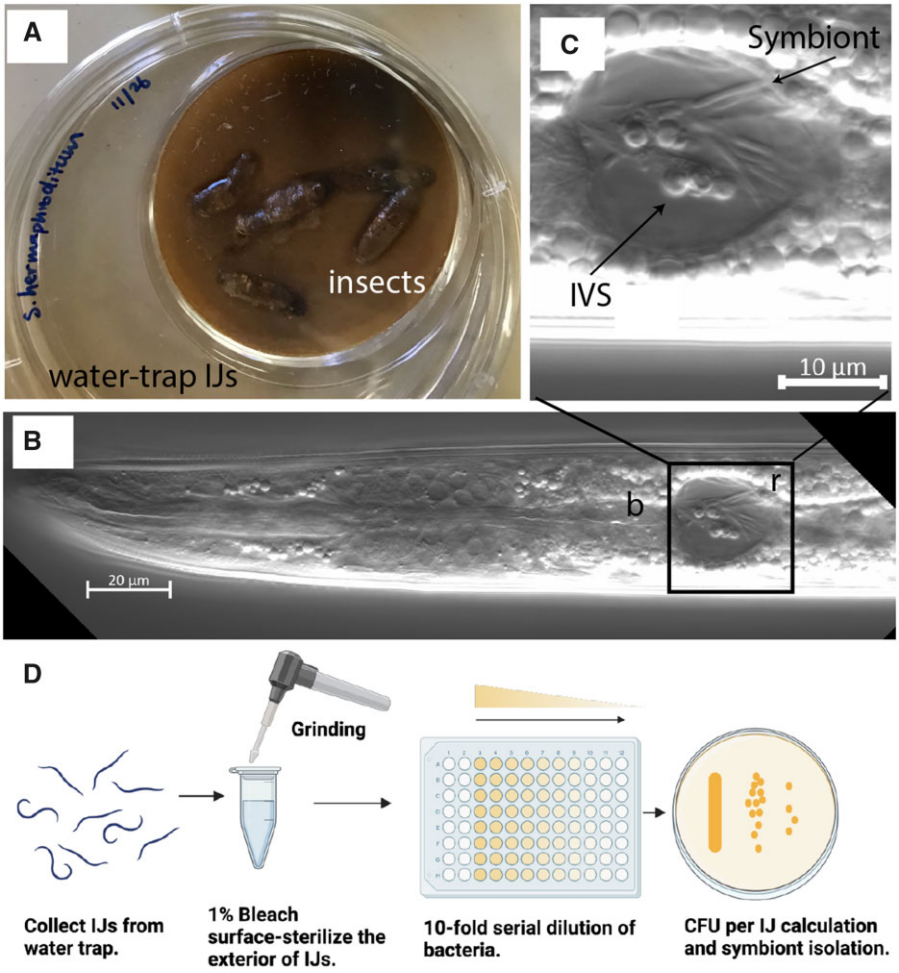

Figure 2 *In vivo* growth of *S. hermaphroditum* and symbiotic bacteria isolation. (A) A modified White trap for the recovery of IJ stage larvae as they disperse from colonized carcasses of *G. mellonella* wax moth larvae. (B) Photomicrograph using Nomarski DIC optics to show the head of an IJ stage *S. hermaphroditum*. Box labeled "r" indicates the receptacle, an intestinal pocket colonized with native symbiotic bacteria. "b" indicates the position of the basal (posterior) bulb of the pharynx. Scale bar, 20 µm. (C) An expanded view of the intestinal vesicle in (B). Rod-shaped symbiotic bacteria are localized in the lumen of the intestinal vesicle. Some bacterial cells adhere to a spherically shaped IVS. Scale bar, 10 µm. (D) Isolation and quantification of symbiotic bacteria that have colonized the intestines of *S. hermaphroditum* IJ larvae. IJs are collected from infected insect hosts, treated with bleach to kill any bacteria on their surfaces, and ground to release bacteria within their intestines. These bacteria are serially diluted until individual colonies can be counted and recovered for further analysis.

scored in individual animals, and homozygosity for one mutation would often make it difficult to score for homozygosity of the other.

Statistics

Animal sizes were compared using the two-tailed unpaired Student's *t*-test. All animal sizes are mean ± SD, $n = 17–20$

Results

Symbiotic bacteria isolation and *in vitro* growth of *S. hermaphroditum*

Consistent *in vitro* growth of nematodes is crucial to optimizing the health, life cycle progression, mating efficiency, and visibility of animals, ultimately facilitating genetic study of the organism (Nigon and Félix 2017). Unlike some other nematodes that could be cultured on a standard *E. coli* lawn on NGM agar, *Steinernema* EPNs usually require their symbiotic bacteria to achieve optimal growth *in vitro* unless they are provided with nontransparent and complex media (Flores-Lara *et al.* 2007; Murfin *et al.* 2012). We collected *S. hermaphroditum* IJs that had emerged from parasitized *G. mellonella* insect larvae and visualized symbiotic bacteria localized in a specialized intestinal pocket termed the receptacle (previously described as the vesicle: Figure 2, A and B; Bird and Akhurst 1983; Kim *et al.* 2012). Contained within the luminal space of the receptacle, some symbiotic bacteria adhere to an intravesicular structure (IVS), an untethered cluster of spherical bodies that has been reported in other *Steinernema* spp. (Figure 2C; Martens and Goodrich-Blair 2005; Sugar *et al.* 2011). To isolate native symbiotic bacteria from *S. hermaphroditum* we first used a 1% bleach solution to sterilize the exteriors of IJs and then extracted their symbiotic bacteria by grinding (Figure 2D). We estimated the average IJ contained 5–10 bacterial CFUs capable of growing on LB-pyruvate agar. *Xenorhabdus* bacteria can exhibit colony-to-colony phenotypic variation that can affect the reproduction of nematodes feeding on them (Boemare and Akurst 1988; Volgyi *et al.* 1998; Park *et al.* 2007; Sugar *et al.* 2011; Cao *et al.* 2017). To examine a range of possible phenotypes from the bacterial extraction, we isolated ten individual colonies as candidate strains for feeding nematodes *in vitro*. Eight isolates produced brown pigment on NGM agar, whereas the other two isolates did not. Similar phenotypic differences in pigment production were reported in other *Xenorhabdus spp* as a signature of phenotypic

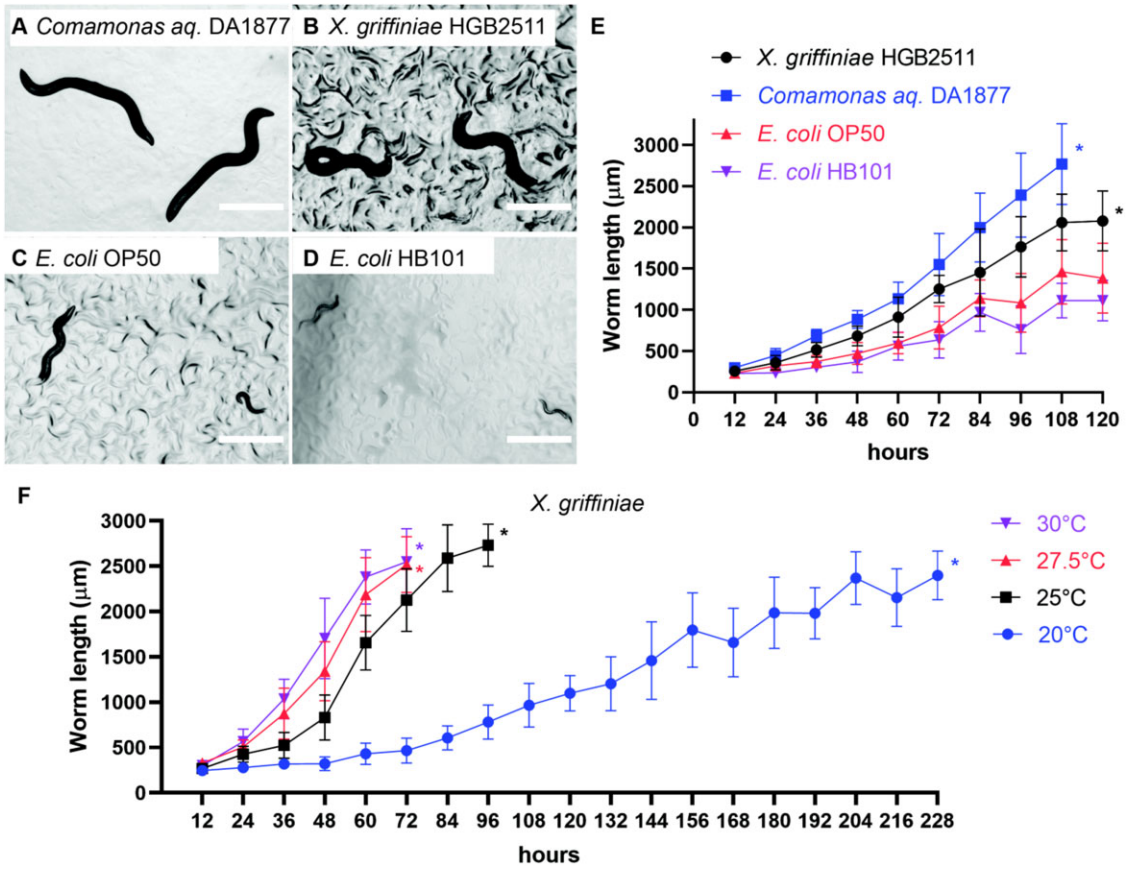

Figure 3 *In vitro* growth of *S. hermaphroditum* PS9179. (A–D) *Steinernema hermaphroditum* embryos free of bacteria were obtained by dissolving gravid adults in bleach solution. The embryos were then seeded on NGM agar plates with lawns of different bacteria as a food source. Images show the sizes of worms that have been grown from embryos at 25°C for 96 h. Scale bars indicate 1 mm. Bacterial lawns were (A) The *S. hermaphroditum* CS34 native symbiont *X. griffiniae* HGB2511; (B) *Comamonas aquatica* DA1877; (C), *E. coli* OP50; (D) *E. coli* HB101.(E, F). Quantification of nematode growth. Body length was measured along the midline of the animal as described in *Materials and Methods*. Asterisks indicate the time point after which the experiment was terminated because animals were obscured by their progeny. (E) Quantification of *S. hermaphroditum* growth on different bacterial lawns on NGM at 25°C. Worms grown on *Comamonas aquatica* were significantly larger than those grown on *X. griffiniae* at every time point ($P < 0.01$, Student's *t*-test), while worms grown on the two *E. coli* lawns were smaller than those grown on *X. griffiniae*, a difference that was statistically significant at every time point except for OP50 at 24 h ($P < 0.05$, Student's *t*-test). Values are mean ± SD ($n = 17$–20). (F) Quantification of *S. hermaphroditum* growth on its native symbiont *X. griffiniae* HGB2511 at different temperatures. *Steinernema hermaphroditum* growth is strongly influenced by temperature. Worms grown at 27.5°C and 30°C were significantly ($P < 0.05$, Student's *t*-test) larger than those grown at 25°C at every time point assayed, whereas worms grown at 20°C were significantly smaller ($P < 0.01$, Student's *t*-test). Values are mean ± SD ($n = 20$)

variation (Sugar *et al.* 2011). To identify the symbiont isolates, we amplified 16S rRNA gene and determined that all 10 isolates had the same sequence, one that is more than 99% identical to the sequence previously reported for *X. griffiniae* strain ID10^T, a symbiotic bacterial strain isolated from a subsequently lost Indonesian isolate of *S. hermaphroditum* (Stock *et al.* 2004; Tailliez *et al.* 2006). Therefore, the phenotypic differences among bacterial isolates are not caused by the coexistence of multiple species of symbiont, but more likely due to phenotypic switching within the same strain, or multiple strains of *X. griffiniae* coexisting in the same natural population of nematode.

To culture *S. hermaphroditum* nematodes *in vitro*, we first compared the growth of these nematodes on their native symbiotic bacteria on three growth media: lipid agar, traditionally used in EPN growth (Vivas and Goodrich-Blair 2001); NGM agar, widely adopted for *Caenorhabditis* and other free-living nematodes (Brenner 1974); and NGM agar supplemented with 0.1% pyruvate, which optimizes the growth of some species of *Xenorhabdus* bacteria (Supplementary Figure S1; Xu and Hurlbert 1990). Symbiotic bacteria grew sufficiently on all three media to support the growth of *S. hermaphroditum*. The nematodes were observed to progress through the stages of their reproductive life cycle (J1-J2-J3-J4-Adult-embryo; see Figure 1B) at a similar pace on all three media in the first generation of growth (Supplementary Figure S1A). Nutrient-rich lipid agar supported growth of a thicker bacterial lawn than did the other two media, and consequently could feed additional generations of nematodes before the bacterial lawn was exhausted. IJs placed on bacterial lawns recovered from developmental arrest and resumed reproductive development on all three media but at slightly different paces (Supplementary Figure S1B). We selected NGM agar as the standard growth condition for genetics study; it is more transparent than lipid agar and supports a thinner bacterial lawn that permits easier visualization and manipulation of the nematodes within it (Figure 3A). To expand our repertoire of *in vitro* growth conditions, we further tested nematode growth feeding on bacterial strains commonly used in the *C. elegans* research community, including *C. aquatica* DA1877 (Figure 3B;Shtonda and Avery 2006; Watson *et al.* 2014), *E. coli* OP50 (Figure 3C; Brenner 1974), and *E. coli* HB101 (Figure 3D;Boyer and Roulland-Dussoix 1969). We found the native symbiont *X. griffiniae* better supported nematode growth *in vitro* than did either of the two *E. coli* strains tested

(Figure 3E). *Steinernema hermaphroditum* nematodes grew faster on *Comamonas* than on their native symbiont (Figure 3E), suggesting that *Comamonas* amply provides nutrients essential for *S. hermaphroditum* development that could be provided by *X. griffiniae* in more limited amounts and are poorly supplied by *E. coli*.

In the laboratory, EPN species have usually been cultured at 20–27°C similar to other soil nematodes (Dunphy and Webster 1989). Our initial trial of breeding *S. hermaphroditum* at room temperature resulted in slow growth (~10 days per generation), whereas higher temperatures supported higher fertility and faster development, consistent with the tropical environment from which they were isolated (Supplementary Figure S1, C and D). At 33°C, the hermaphrodites cannot produce living embryos, whereas 37°C causes lethality of the animals (Supplementary Figure S1, C and D). To better optimize the growth temperature, we monitored nematode growth under various temperatures from 20°C to 30°C (Figure 3F). *Steinernema hermaphroditum* CS34 showed a range of generation times: roughly 2.5 days at 30°C, 3 days at 27.5°C, 4 days at 25°C, and more than 9 days at 20°C. The generation time at 25–30°C is similar to the generation time of *C. elegans* growth in the laboratory at its optimal cultivation temperature. We used 25°C as a standard growth condition for *S. hermaphroditum* to facilitate the adaptation of breeding and genetic techniques developed for use in *C. elegans*.

Establishing a protocol for cryopreservation of *S. hermaphroditum*

The short generation time of nematodes and the lack of outbreeding in a selfing hermaphrodite mean that continuously cultured *S. hermaphroditum* would accumulate mutations and might rapidly show inbreeding depression (Dolgin *et al.* 2007). Cryopreservation is therefore a crucial technique to maintain healthy lines. To develop a cryopreservation method, we first attempted to freeze *S. hermaphroditum* IJs adapting a methanol-wash protocol that has been previously adopted in multiple *Heterorhabditis* and *Steinernema* species (Popiel and Vasquez 1991) but failed to consistently recover viable nematodes from frozen stocks. An attempt using a glycerol-based freezing protocol adapted from *C. elegans* research gave a low yield of viable *S. hermaphroditum* that survived freezing (5–20 nematodes per ml; Supplementary Table S2). We more successfully adapted a recently reported trehalose-DMSO protocol for freezing *C. elegans* (O'Connell 2021). Using this protocol we efficiently froze and recovered *S. hermaphroditum* mixed stage juveniles (Supplementary Table S2). Nematodes grown on NGM showed better survival (>200 nematodes survived per ml) than did those grown on lipid agar (5–20 nematodes per ml), suggesting the two growth conditions may cause drastic physiological differences. The frozen stock was test-thawed over the course of 2 months and was found to provide stable, highly efficient recovery. We used the resulting trehalose-DMSO freezing protocol for the cryopreservation of *S. hermaphroditum* strains in this research.

Establishing a homozygous and stable isogenic line via inbreeding

A population of nematodes isolated from the wild is likely to contain a mix of genotypes and to be heterogeneous in genome sequences (Barrière and Félix, 2006). To facilitate future genome sequence assembly and to provide a genetically and phenotypically consistent population for genetic study, it is useful to obtain a homozygous and stable isogenic line via inbreeding (Barrière and Félix 2006). *Steinernema hermaphroditum* was not previously known to be hermaphroditic after the first generation (Stock *et al.* 2004): male–female reproduction is more likely to cause inbreeding depression when immediately isolating single mating pairs. We therefore adopted an inbreeding strategy appropriate to a male–female population by first establishing ten mating groups of nematodes cocultured with ten symbiotic bacterial isolates (Ancestral groups I to X corresponding to symbiotic bacteria isolates 1–10, respectively, Supplementary Figure S2; Barrière and Félix 2006). We discovered that feeding on the eight pigmented (brown) bacterial isolates (Ancestral groups I, II, III, V, VI, VIII, IX, and X) produced relatively higher progeny numbers, while feeding on either of the nonpigmented bacterial isolates (Ancestral groups IV and VII) produced relatively fewer progeny (data not shown). We chose five ancestral lines including both pigmented and nonpigmented symbionts (Ancestral groups III, IV, VI, VII, and IX) for further inbreeding by isolating ten single mating pairs from each of the five ancestral lines. During this process of inbreeding, we observed a low (<5%) frequency of males in the population and found that the animals with a grossly female appearance could consistently reproduce when males were absent (see details below). Having found that the *S. hermaphroditum* wild isolate CS34 is stably hermaphroditic or parthenogenic for multiple generations, we inbred the wild-type line by isolating single self-reproducing virgin juvenile hermaphrodites for 5–10 consecutive generations on various lines of symbiotic bacteria (Supplementary Figure S2 and Table S1). One strain, PS9179, derived from ancestral line IX, inbred by selfing single animals for ten generations cocultured with the pigmented bacterial isolate HGB2511, was chosen to function as a reference strain; all subsequent work was done with PS9179 nematodes cultured on NGM with HGB2511 bacteria. Animals of this strain are healthy and active, and have retained their ability to infect and kill *G. mellonella* insect larvae and reproduce in the resulting carcass, eventually producing a new generation of IJs.

Steinernema hermaphroditum is consistently hermaphroditic

Next, we examined if sperm was present in unmated animals with female-like somatic morphology, which would be evidence of hermaphroditism. We dissected the gonads of virgin hermaphrodites and observed sperm-like objects in a region of the gonad that corresponds to the spermatheca of other species (Figure 4, C and D). The sperm-like objects (Figure 4E) were shown to be nucleated when stained for DNA with DAPI (Figure 4F), and were strikingly small in size when observed using differential interference contrast (DIC) microscopy (~1.5 μm diameter), which may be a reflection of differences in spermatogenesis (LaMunyon and Ward 1998; Vielle *et al.* 2016; Winter *et al.* 2017). To confirm that these small cells were indeed sperm, we applied an antibody that recognizes MSP. MSPs are small, highly conserved proteins in nematode sperm and are thought to have cytoskeletal and signaling functions (Roberts and Stewart 1995; Miller *et al.* 2001). The monoclonal antibody was generated against the last 21 amino acids of the *C. elegans* protein MSP-40 (Miller *et al.* 2001) and has been successfully applied to *Acrobeloides* nematodes (Heger *et al.* 2010) which are in the same clade (IV) as *Steinernema* (Schiffer *et al.* 2018). To confirm that MSP is conserved in *Steinernema spp*, we used WormBase ParaSite (Bolt *et al.* 2018) to search for *C. elegans* MSP-40 homologs in *Steinernema carpocapsae*, the *Steinernema* species with the most complete genome (Dillman *et al.* 2015; Rougon-Cardoso *et al.* 2016; Serra et al. 2019). We found seven *msp* homologs in *S. carpocapsae* with 68.7–91.3% overall amino acid sequence identity to *C. elegans* MSP-40.

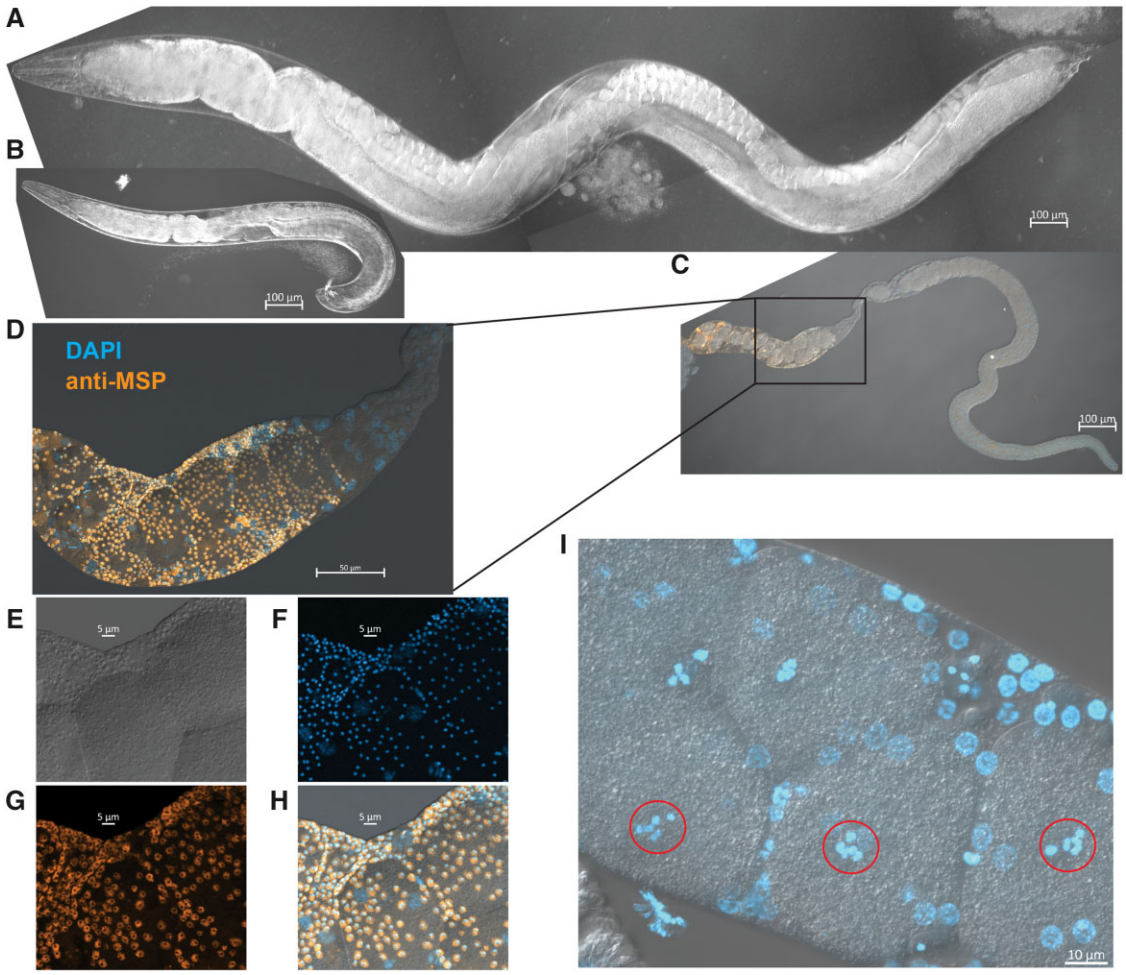

Figure 4 *Steinernema hermaphroditum*-India is consistently hermaphroditic. Progeny of an unmated *S. hermaphroditum* hermaphrodite consist mostly of hermaphrodites but also include rare males. (A) An adult hermaphrodite of *S. hermaphroditum*. Scale bar, 100 µm. (B) An adult male of *S. hermaphroditum* at the same magnification. Scale bar, 100 µm. (C) A dissected gonad arm from a young hermaphrodite stained with the DNA dye DAPI (blue) and with an antibody against MSP (orange). Scale bar, 100 µm. (D) A section of the gonad arm shown in (C) with higher magnification showing the presence of sperm (orange) in the spermatheca of an unmated hermaphrodite. Scale bar, 50 µm. (E–H) Higher magnification images of a section of the spermatheca showed in (D). (E) Nomarski microscopy (DIC); (F) DAPI; (G) Anti-MSP; (H) Merged. Scale bars, 5 µm. (I) Oocytes in diakinesis show five pairs of tetraploid chromosomes at Meiosis Prophase I (red circles). Scale bar, 10 µm.

Most importantly, the C-terminal 21 amino acids used to generate the monoclonal antibody, we had used (REWFQGDGMVRRKNLPIEYNP) were 100% identical. We therefore expected that the sperm of *S. hermaphroditum* would contain this highly conserved antibody epitope and would be identified by antibody staining. Indeed, the small cells in the gonads of unmated animals with a female somatic appearance were confirmed by anti-MSP antibody staining to be hermaphroditic sperm. Thus, the structure they reside in is a spermatheca and the animal is hermaphroditic (Figure 4, D, G, and H).

Altogether, we conclude that *S. hermaphroditum* is consistently hermaphroditic. Each generation consists almost exclusively of self-reproducing hermaphrodites, accompanied by spontaneous males. The mode of reproduction could be either self-fertilization (similar to that of *C. elegans*) or parthenogenesis.

Forward genetic screens in *S. hermaphroditum* result in mutants with a wide variety of phenotypes

The consistent hermaphroditism of selected nematodes, in particular *C. elegans*, greatly facilitated the development of genetic tools (Brenner 1974). Our discovery of the first consistently hermaphroditic EPN motivated us to immediately develop forward-genetic tools in *S. hermaphroditum*. We adapted and optimized EMS mutagenesis protocols used on *C. elegans* to screen for mutant lines of *S. hermaphroditum*. A series of trial screens produced over three hundred candidate mutant animals resulting in at least 37 independent mutant lines with visible and stable phenotypes with mostly 100% penetrance. The mutants showed a wide variety of phenotypes including dumpy (Dpy), various types of uncoordinated locomotion (Unc), gonad migration defective (Mig), a strain whose larvae develop as IJs before resuming reproductive development (dauer-constitutive, Daf-c), and a high-incidence-of-males (Him) strain that has reduced brood size and produces sick, slow-growing animals (Figure 5 and Table 1). Mutant strains were tested by mating with wild-type males to determine whether their phenotype was dominant or recessive; three strains could not be tested because of a highly variable phenotype or because they could not be successfully mated. Nearly, all mutant phenotypes tested were recessive; the one exception, *unc(sy1654)*, had a recessive strong locomotion defect and a dominant phenotype that caused it to continuously twitch, strongly

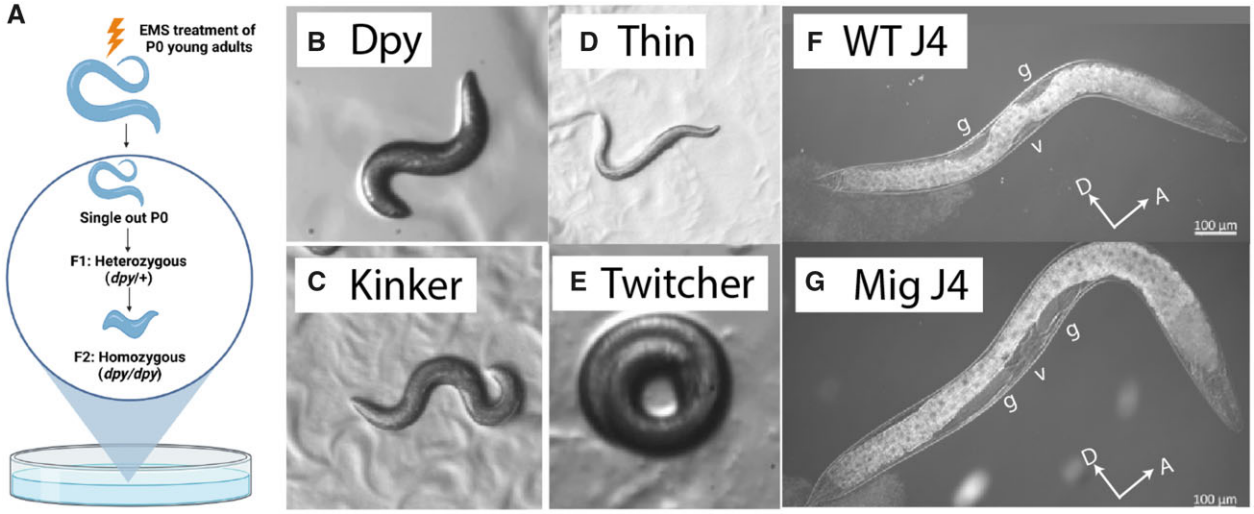

Figure 5 EMS mutagenesis of *S. hermaphroditum*. (A) EMS mutagenesis of young adults (the P_0 or parental generation) and isolation of mutant lines from individuals in the F_2 generation. Candidate mutant strains are tracked to identify the mutagenized P_0 animal they descended from (B–G) examples of mutant phenotypes. (B) The dumpy appearance of *dpy(sy1646)*. (C) The resting posture of the uncoordinated mutant *unc(sy1636)*, a kinker Unc. (D) The long, thin uncoordinated mutant *unc(sy1653)*. (E) The twitcher mutant *unc(sy1654)*; see also a film of its phenotype in Supplementary materials. (F) Wild type (WT) fourth-stage J4 larva. The developing gonad starts on the ventral side near the animal's midpoint (labeled "v") and expands both anteriorly and posteriorally. As the gonad expands it pushes aside the intestine (which has a white appearance), resulting in clear patches (labeled "g"). It can be seen that the gonad has moved dorsally both anterior and posterior to its starting point. Anterior is to the right and dorsal is up. Scale bar, 100 µm. (G) Altered gonad migration is apparent in the J4 stage of a *mig(sy1637)* mutant. Note that the expanding gonad has remained entirely ventral as it has expanded to the anterior and the posterior of its starting point (labeled "v"). Anterior is to the right and dorsal is up. Scale bar, 100 µm. "A" denotes anterior; "D" denotes dorsal; "v" indicates the position of vulva; and "g" indicates the position of gonad arms.

resembling loss-of-function mutants of the *C. elegans* gene *unc-22* (Moerman and Baillie 1979). The predicted proteome of the related nematode *S. carpocapsae* (Serra *et al.* 2019) contains one sequence sharing 67% identity with *C. elegans* UNC-22 over 5169 amino acids. Previously, mutants of *unc-22* orthologs in other nematodes in the same clade as *Steinernema* (IV) caused twitcher phenotypes resembling those of *C. elegans unc-22* mutants (Link *et al.* 1987; Gang *et al.* 2017).

The progeny of crosses between wild-type males and mutant hermaphrodites were predominantly self-progeny rather than cross progeny, indicating that unlike what is observed in some other hermaphroditic nematodes such as *C. elegans* (Ward and Carrel 1979) sperm introduced by mating with a male do not preferentially produce cross progeny in mated animals.

Steinernema hermaphroditum is androdioecious with chromosomal sex determination

Crosses of mutant hermaphrodites with wild-type males also revealed that sex determination in *S. hermaphroditum* is chromosomal: for 7 of 27 mutants, mating with wild-type males produced wild-type hermaphrodite cross progeny and mutant male cross progeny, in approximately equal numbers, indicating these markers are X-linked. For two independently recovered X-linked *dpy* mutants, these ratios were counted and found to be 47 hermaphrodites: 41 males (*sy1644*), and 116 hermaphrodites: 115 males (*sy1646*).

When double-mutant hermaphrodites homozygous for the autosomal mutation *him(sy1680)* and the X-linked recessive marker *unc(sy1635)* X were mated with wild-type males, phenotypically wild-type (non-Unc) male progeny were observed. A similar mating of wild-type males with *unc(sy1635)* X hermaphrodites produced cross-progeny that were all *unc(sy1635)* X/+ wild-type hermaphrodites and *unc(sy1635)* X/0 males; the observed non-Unc males from the cross with *him(sy1680)*; *unc(sy1635)* X hermaphrodites could only be explained by their containing a paternal wild-type X chromosome and not containing an *unc(sy1635)*-marked maternal X chromosome. This observation indicates that the high-incidence-of-males phenotype of *sy1680* results from X chromosome loss in oogenesis, further demonstrating the chromosomal nature of sex determination in *S. hermaphroditum*.

Although *S. hermaphroditum* animals consistently produce progeny without being mated, this is not enough to prove that it is a self-fertilizing hermaphrodite; an alternative explanation is that they could be producing self-progeny through parthenogenesis. One way to test this is by examining the progeny of a heterozygous animal: if multiple markers show Mendelian ratios, this excludes the parthenogenesis model (see Figure 6). To further examine if *S. hermaphroditum* is parthenogenic or self-fertilizing, we examined the self-progeny of animals heterozygous for each of several mutants with strong, easily detected mutant phenotypes. The F_2 progeny of all mutants so examined segregated according to a Mendelian ratio (Table 2). In particular, two pairs of mutations—*dpy(sy1639)* and *unc(sy1635)*, and *unc(sy1647)* and *dpy(sy1652)*—are each on the same chromosome and not closely linked to each other on their shared chromosome (~17 map units and 20 map units, respectively; data in Figure 7); all four markers showed Mendelian segregation (Table 2). These results are consistent with hermaphroditism by self-fertilization, and are not consistent with parthenogenesis.

Identification of linkage groups in *S. hermaphroditum*

DAPI staining of gonads showed five pairs of tetraploid chromosomes in diakinesis stage oocytes (Figure 3E), which is consistent with the chromosome numbers reported for other *Steinernema* species (Curran 1989). We have begun using our collection of *S. hermaphroditum* mutants to generate the first genetic linkage map of an EPN (Figure 7 and Table 1). Genetic mapping has shown that mutations on the X chromosome are linked to each other

Table 1 Description of mutant strains and alleles

Strain	Allele	Phenotype	Linkage group	Description
PS9258	*mig(sy1637)*	Gonad migration defective	I	
PS9255	*dpy(sy1634)*	Dumpy, Vulvaless	Unknown	Lack of vulva prevents mating
PS9256	*unc(sy1635)*	Uncoordinated	X	Reverse kinker
PS9257	*unc(sy1636)*	Uncoordinated	III	Kinker; Fails to complement *unc(sy1647)*
PS9260	*dpy(sy1639)*	Dumpy	X	Fails to complement *dpy(sy1644)* and *dpy(sy1646)*
PS9265	*dpy(sy1644)*	Dumpy	X	Fails to complement *dpy(sy1639)* and *dpy(sy1646)*
PS9267	*dpy(sy1646)*	Dumpy	X	Fails to complement *dpy(sy1639)* and *dpy(sy1644)*
PS9268	*unc(sy1647)*	Uncoordinated	III	Kinker; fails to complement *unc(sy1636)*
PS9269	*daf(sy1648)*	Dauer-constitutive	II	
PS9270	*unc(sy1649)*	Uncoordinated	Autosomal	Kinker. Slow growth.
PS9272	*unc(sy1651)*	Uncoordinated	Autosomal	Kinker
PS9273	*dpy(sy1652)*	Dumpy	III	
PS9274	*unc(sy1653)*	Uncoordinated	X	Kinker
PS9275	*unc(sy1654)*	Uncoordinated	I	Dominant twitcher, recessive lethargic
PS9276	*unc(sy1655)*	Uncoordinated	III	Reverse kinker
PS9277	*dpy(sy1656)*	Small body size	Autosomal	
PS9278	*unc(sy1657)*	Uncoordinated	X	Reverse kinker
PS9279	*dpy(sy1659)*	Dumpy	Autosomal	
PS9282	*unc(sy1661)*	Uncoordinated	Autosomal	Loopy
PS9283	*dpy(sy1662)*	Dumpy	X	Complements *dpy(sy1639)*, *dpy(sy1644)*, and *dpy(sy1646)*
PS9285	*dpy(sy1664)*	Dumpy	I	
PS9287	*dpy(sy1666)*	Dumpy	Unknown	No cross progeny from mating
PS9288	*unc(sy1667)*	Uncoordinated	I	Lethargic, rigid posture
PS9289	*unc(sy1668)*	Uncoordinated	II	Lethargic, rigid posture
PS9290	*unc(sy1669)*	Uncoordinated	I	Kinker
PS9291	*dpy(sy1670)*	Dumpy	Autosomal	
PS9293	*unc(sy1672)*	Uncoordinated	I	Reverse kinker
PS9294	*mig(sy1673)*	Gonad migration defective	III	
PS9295	*unc(sy1674)*	Uncoordinated	Autosomal	Kinker
PS9296	*dpy(sy1675)*	Dumpy	II	
PS9300	*unc(sy1679)*	Uncoordinated	Unknown	Loopy, variable phenotype
PS9301	*him(sy1680)*	High incidence of males	Autosomal	Variable sickness, low brood size

A list of mutant *S. hermaphroditum* strains recovered in this work. Each mutant was recovered from different mutagenized P_0 animals than any other mutant with the same allele number; this includes one set of three mutants and another set of two mutants that fail to complement each other. Linkage group assignment was determined as described in *Materials and Methods* and as shown in Figure 5.

and has thus far identified three autosomal linkage groups; mapping additional markers is expected to generate a map that matches our cytological observations.

Discussion

In this research, we report that a recently isolated Indian strain of *S. hermaphroditum* CS34 is consistently hermaphroditic. We have produced a highly inbred line of *S. hermaphroditum* to support molecular analysis and provide a consistent phenotypic basis for experimentation. The capacity for parasitism is retained in the inbred line, which remains able to efficiently infect and kill insect larvae in partnership with its *X. griffiniae* bacterial symbiont. We confirmed that hermaphrodites of this strain contain sperm and reproduce by self-fertilization, and can also be mated by males. EMS mutagenesis of this strain generated mutant lines that consistently demonstrate a variety of phenotypes and serve as genetic markers to demonstrate chromosomal sex determination and create an initial genetic linkage map of *S. hermaphroditum*.

Previous research characterized *S. hermaphroditum* as hermaphroditic in the first generation recovered from insects. Because of the culture methods used, it had not been possible to determine whether subsequent generations developed as self-fertile hermaphrodites or as females (Griffin *et al.* 2001; Stock *et al.* 2004). It was observed that animals of the second generation that were grossly female in somatic morphology lacked a visible spermatheca (Stock *et al.* 2004). Other EPNs capable of producing self-fertile hermaphrodites develop as females in subsequent generations (Dix *et al.* 1992). We discovered that *S. hermaphroditum* CS34 develops consistently as self-fertile hermaphrodites in every generation, and that unmated animals with a female somatic morphology contain sperm.

Traditional EPN *in vitro* growth methods using lipid agar and liver-kidney agar have been widely applied in nematology and microbial symbiosis research. These rich media could support nematode growth either with symbiotic bacteria or, in the latter case, without bacteria (axenically; Surrey and Davies 1996; Vivas and Goodrich-Blair 2001; Flores-Lara *et al.* 2007) and facilitated the description of the animals and the mass production of nematodes, especially IJs. However, they also hampered the application of basic techniques required for molecular and experimental genetics. The presence of animal tissue in the media decreases visibility of the nematodes, while oil droplets hamper nematode picking and cause inconsistency through variable distribution in the media. We adapted standard growth conditions (NGM) for laboratory culture of the free-living soil nematode *C. elegans* to grow both *S. hermaphroditum* and its *Xenorhabdus* bacterial symbiont and demonstrated that basic techniques developed in *C. elegans* could be adapted to this EPN. Our purpose in adopting *C. elegans* techniques is to encourage the application of approaches from multiple research traditions to better serve various functions in a broader research community.

Xenorhabdus bacteria undergo phenotypic switching: pleiotropic variation of observable phenotypes such as secondary metabolite production and motility (1°–2° form; Boemare and Akurst

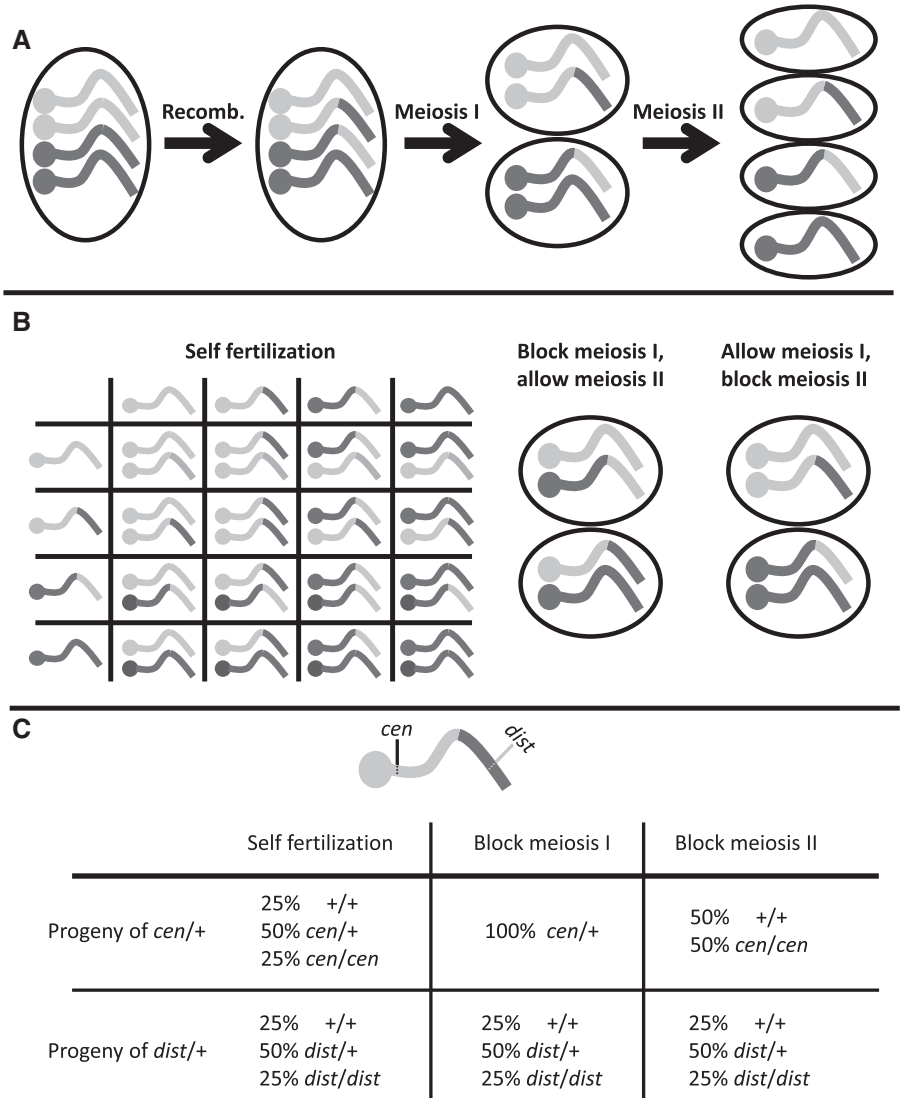

	Self fertilization	Block meiosis I	Block meiosis II
Progeny of *cen*/+	25% +/+ 50% *cen*/+ 25% *cen*/*cen*	100% *cen*/+	50% +/+ 50% *cen*/*cen*
Progeny of *dist*/+	25% +/+ 50% *dist*/+ 25% *dist*/*dist*	25% +/+ 50% *dist*/+ 25% *dist*/*dist*	25% +/+ 50% *dist*/+ 25% *dist*/*dist*

Figure 6 Parthenogenesis *vs* self-fertilizing hermaphroditism. Animals that have a grossly female appearance and that can reproduce without being mated might be producing progeny by self-fertilization or might be parthenogenic. The differences between these modes of reproduction would affect the suitability of the organism for genetic studies. (A) Normal meiosis is shown diagrammatically for a single chromosome, with its centromere visible in the cartoon as a ball at the left end of the chromosome. This diploid animal has a pair of homologous chromosomes; one is shown as light in color, and one is shown as dark, representing their different haplotypes. Mitotic DNA replication has doubled the number of chromosomes during oogenesis. Each homologous chromosome is present in two copies of sister chromatids forming a tetraploid bivalent chromosome pair similar to Figure 4I. Recombination can occur at this stage to cause the exchange of sections of the chromosome sequences distal to the site of crossing over with respect to the centromere, as shown for one pair in this cartoon. In Meiosis I, the two homologous chromosomes are separated from each other, and in Meiosis II the individual sister chromatids are separated from each other. (B) In self-fertilization, a diploid embryo is generated by fusion of two haploid gametes produced by separate meiosis in oogenesis and spermatogenesis. In parthenogenesis, no sperm fertilizes the oocyte. The diploid embryo is produced by preventing the reduction of chromosome number in meiosis I or meiosis II in the oocytes. Examples are shown of the progeny classes that could result from this; focus on the different sorting of the centromeres into zygotes. (C) If we consider two markers, one tightly linked to the centromere (*cen*) and one (*dist*) distant from the centromere and genetically unlinked to it, and so recombinant with respect to the centromere half of the time, we can then examine the resulting progeny frequencies assuming the mechanisms shown in (B) for the distal marker *dist* that isn't genetically linked to the centromere no difference will be observed between mechanisms, but for the centromere-linked marker *cen* there will be a marked difference: 25% of self-fertilized embryos will be homozygous, but depending on the mechanism of parthenogenesis either 0% or 50% of progeny will be homozygous close to the centromere.

1988) and virulence modulation, in which individual cells can become attenuated for virulence in insects (Park *et al.* 2007), each of which can affect interactions between bacteria and nematodes. *Steinernema carpocapsae* newly isolated from the wild are reported to associate exclusively with the 1° form of their *X. nematophila* symbiont (Forst *et al.* 1997). In virulence modulation, virulence-attenuated-phase bacteria colonize their nematode host and support its reproduction better than do the same bacterial species in a more virulent phenotypic phase (Cao *et al.* 2017). In this research, we isolated ten colonies of symbiotic bacteria *X. griffiniae* from a natural population of *S. hermaphroditum* IJs and found the production of brown pigment varied among the isolates. Pigmented bacteria supported nematode reproduction better than nonpigmented isolates did, suggesting potentially important consequences of phenotypic switching in this species. The various phenotypes of individual isolates of symbiotic bacteria that have correspondingly different impacts on the physiology of their host nematodes provoke intriguing questions about the possible

Table 2 Segregation of selected genetic markers from heterozygotes in self-reproduction

Marker	Proportion of self-progeny with abnormal phenotype (%)
unc(sy1635) X	17/61 (28)
	30/120 (25)
dpy(sy1639) X	38/136 (28)
	38/159 (24)
	29/123 (24)
	30/117 (26)
dpy(sy1644) X	25/90 (28)
	12/68 (18)
	29/132 (22)
dpy(sy1646) X	62/267 (23)
	25/106 (24)
unc(sy1647) III	26/107 (24)
	14/69 (20)
	29/102 (28)
	33/155 (21)
	37/148 (25)
	33/125 (26)
dpy(sy1652) III	23/90 (26)
	28/108 (26)
dpy(sy1664) I	19/101 (19)
	33/139 (24)
	30/112 (27)

Animals heterozygous for various recessive markers were selfed and their progeny were sampled to determine what proportion were homozygous for the marker. In every case, that proportion was close to one in four. This is the result to be expected from self-fertilization; it is not consistent with parthenogenesis (see Figure 6). Note in particular that two pairs of these markers—*unc(sy1635)* and *dpy(sy1639)*, and *unc(sy1647)* and *dpy(sy1652)*—are ~20 map units apart on the same chromosome, suggesting that they cannot both be far distant from the centromere, as would be required to explain this proportion in parthenogenic reproduction.

heterogeneity of both nematode and bacteria in natural populations. Alternatively, multiple closely related strains of *X. griffiniae* could also exhibit variable pigment production within a natural population of nematodes. However, if there were distinct strains rather than phenotypic variation, they were not be distinguishable by 16S rRNA sequencing we performed.

The ability of *Xenorhabdus* bacteria to support the reproduction of their native host *Steinernema* nematodes is a crucial aspect of their mutualistic relationship (Herbert and Goodrich-Blair 2007). We monitored *S. hermaphroditum* growth using as its food source either its native symbiont or three bacterial strains commonly used in *C. elegans* research. The ability of *E. coli* (OP50 and HB101) to support the development of *C. elegans* but not to robustly support *S. hermaphroditum* growth indicates these two bacteriovorous nematode species may have different nutritional needs or food preferences as a result of their distinct life styles (free-living *vs* parasitic). Unexpectedly, we discovered that a nonsymbiotic bacterial species *C. aquatica* could support nematode growth better than its native symbiotic bacterium *X. griffiniae*. Therefore, *C. aquatica* could serve as a neutral (nonpathogenic and nonmutualistic) food source for *S. hermaphroditum*. However, the advantage of *Comamonas* in supporting *S. hermaphroditum* growth *in vitro* does not necessarily mean *Comamonas* would be a better partner in the wild. First, the *in vitro* growth conditions may not represent those *in vivo*. The insect carcasses are normally rich sources of nutrients and the EPNs would therefore have less need for their bacteria to abundantly produce those nutrients; also, the insect carcass might better enable the *X. griffiniae* metabolism to support nematode growth than does the agar media used in our assays. Even more importantly, *Xenorhabdus* bacteria contribute to insect-killing and help protect the carcass from other predators and other microbial species by producing inhibitory molecules, such as toxins and secondary metabolites with antimicrobial effects (Herbert and Goodrich-Blair 2007). The antagonizing mechanisms protect the bacterial and nematode partners from exposure to potentially invasive microbes and ensure the fitness and fidelity of their mutualistic symbiosis (Herbert and Goodrich-Blair 2007). These antagonizing mechanisms of the bacteria may also moderately inhibit nematode growth. Future research can take advantage of the unique binary symbiosis system of *S. hermaphroditum* and *X. griffiniae* to investigate the role of native symbionts and other environmental microbes at different stages of the symbiotic life cycle, such as nematode-bacteria signaling during the infective stage. As *S. hermaphroditum* is developed as a genetic model it will be possible to study the mechanisms that tie these two symbiotic partners together, experimentally modifying both partners in the interaction.

We found EMS mutagenesis to be an efficient way of recovering mutant *S. hermaphroditum* strains with highly specific defects in diverse aspects of their biology. Mutants could easily be maintained and could be used to demonstrate a number of basic but essential features of this species. We found that sex is determined chromosomally, by the presence or absence of a second X chromosome. Sex determination appears to be XX/XO as opposed to XX/XY, because hermaphrodites can spontaneously generate male progeny. In addition, we showed that a Him mutant greatly increased the frequency of spontaneous male progeny by generating oocytes that lacked an X chromosome. By mating wild-type males to mutants with recessive phenotypes that allowed the identification of cross-progeny we demonstrated that *S. hermaphroditum* does not exhibit a strong preference for the use of male-derived sperm. This phenomenon has been a notable feature of *C. elegans* biology and has been proposed to promote the small amount of outcrossing necessary to prevent uniformity in an inbred population (Ward and Carrel 1979). Critically for future genetic research using *S. hermaphroditum*, we could use visibly phenotypic mutants to show that self-progeny are produced by fertilization with sperm that the hermaphrodites produce, rather than by parthenogenesis. In parthenogenesis, the cell that would normally develop into a haploid oocyte instead becomes a diploid zygote, without being fertilized by sperm. Different mechanisms can achieve this result, including preventing the reduction of chromosome number at meiosis I or meiosis II; any such mechanism will result in different frequencies of homozygotes segregating from a mother heterozygous for a marker, depending on the genetic distance between that marker and the chromosome's centromere (Figure 6). We found that for every marker tested, including two pairs of markers distant from each other on the same chromosomes, homozygotes were one quarter of the progeny—a Mendelian ratio that is the hallmark of self-fertilization. This ensures that it will be possible to screen efficiently for recessive phenotypes at all points in the genome.

The collection of mutants we have already assembled is sufficient to describe how sex is determined in *S. hermaphroditum* and offers a proof of principle of the potential of forward genetic screens in this organism. Future screens will be able to target biological questions involving the unique biology of the EPN, such as the recognition, maintenance, and transmission of its mutualistic symbiont and its ability to hunt and to parasitize insects. Already

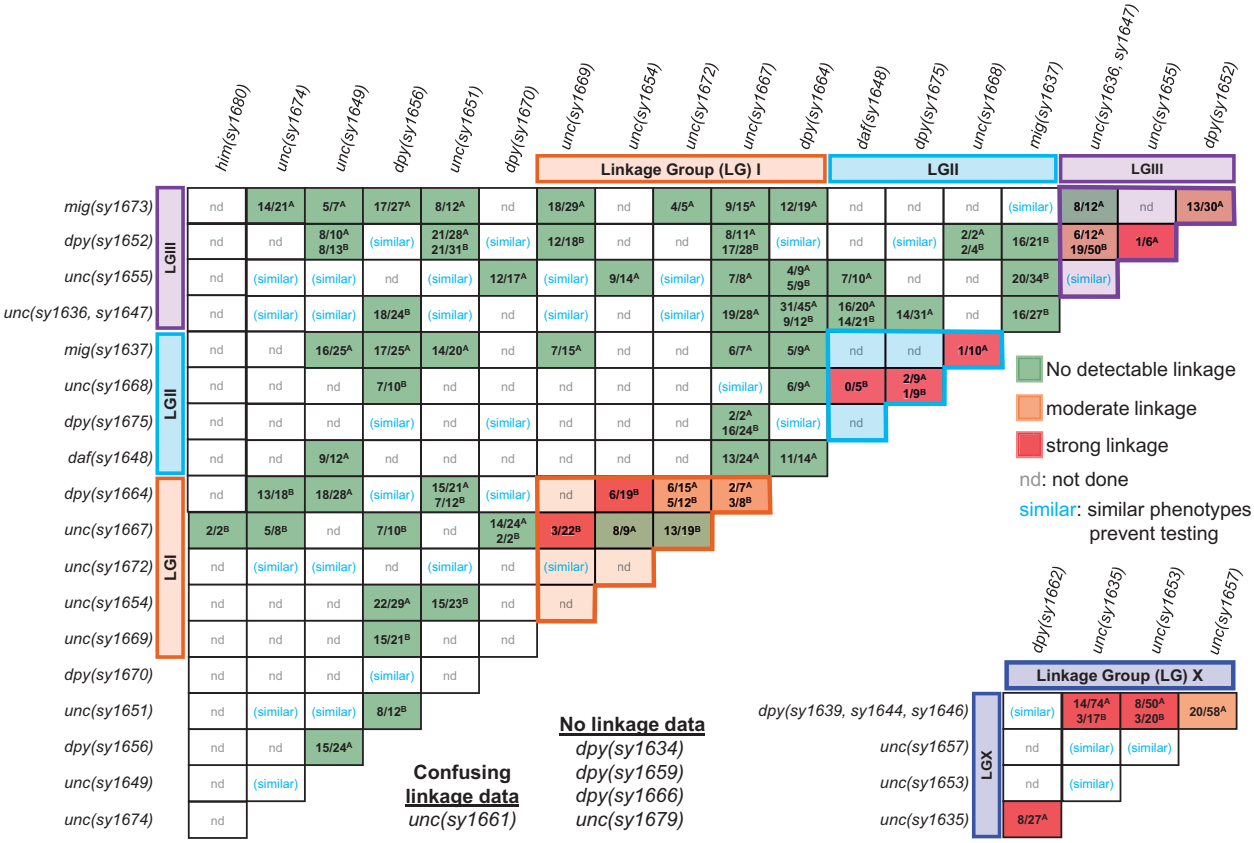

Figure 7 A first linkage table for *S. hermaphroditum*. Genetic markers were mapped as described in *Materials and Methods*. Numbers shown are the proportion of homozygotes for a first marker whose progeny included animals showing the phenotype of a second marker; superscript "A" indicates the first marker was the mutation listed at left, labeling the row; superscript "B" indicates the first marker was the mutation listed above, labeling the column. Mapping results are colored to indicate strength of linkage: results consistent with unlinked (approximately two-third of animals homozygous for a first marker produced progeny phenotypic for a second marker) are green, results consistent with stronger linkage (less than one-third) are in red. Intermediate animals (one-third or more, but significantly less than two-third) are in orange. Some mutations were difficult to score reliably, giving confusing results (*unc(sy1661)*, not included in the mapping data shown) or could be difficult to detect, giving the false impression of linkage [*dpy(sy1675)*, specifically in combination with *unc(sy1636)*]. Seven mutations were assigned to the X chromosome, and were linked to each other on that chromosome; 20 autosomal mutations have thus far defined three linkage groups, of an expected four. LG, Linkage Group.

we have a couple of interesting mutants: one that in every generation causes its progeny to transiently develop as IJs rather than prioritize reproduction, and two unlinked mutations sharing a novel phenotype of altered gonad shape that may reveal fundamental mechanisms of cell migration. Development of transgenesis and of reverse-genetics tools such as RNAi and CRISPR-Cas9 genome editing should expand a genetics toolkit we have begun to build by exploring gene function through forward genetics. Engineered nucleases such as CRISPR-Cas9 can also be used to build the tools that will make forward genetics more powerful (Dejima *et al.* 2018). The availability of a complete and annotated *S. hermaphroditum* genome would greatly facilitate both the targeting of genes for reverse genetics and the identification of genes mutated in forward genetic studies. We hope that the discovery of additional wild isolates of *S. hermaphroditum* will facilitate genetic mapping in this species, enable the study of this species' natural diversity, potentially including molecular pathways underlying sex determination, and comparative study among free-living and parasitic nematodes.

Data availability

Strains described in this work are available upon request. 16S rRNA gene sequences of the *X. griffiniae* bacterial symbionts of the *S. hermaphroditum* isolate CS34 are available in the Genbank database. The accession numbers for 16S rRNA sequence (including HGB2511) are MZ913116–MZ913125. Supplemental material is available at figshare: https://doi.org/10.25386/genetics.16689217.

Acknowledgments

We are overwhelmingly grateful for *S. hermaphroditum* as a generous gift from nature and a superb organism to explore scientific curiosities. We thank Adler Dillman of University of California Riverside for generously sharing the *S. hermaphroditum*-India strain CS34 and for comments on this manuscript. We also thank Heidi Goodrich-Blair and Jennifer Heppert of the University of Tennessee Knoxville for helpful discussions and editorial suggestions. We are also grateful for valuable suggestions from Zuzana Kocsisova. We appreciate our correspondence with Christine Griffin on the mode of reproduction of *S. hermaphroditum*-Indonesia. The monoclonal anti-MSP antibody 4A5 developed by David Greenstein of the University of Minnesota was obtained from the Developmental Studies Hybridoma Bank, created by the NICHD of the NIH and maintained at The University of Iowa Department of Biology. Bacterial strains HB101 and DA1877 were obtained from the *Caenorhabditis* Genetics Center (CGC), which is funded by the NIH Office of Research Infrastructure Programs

(P40 OD010440). This work was also facilitated by WormBase and ParaSite, a knowledgebase for nematode research. Figures 2D and 5A are created with BioRender.com.

Funding

This research was supported by National Institutes of Health (NIH) Ruth L. Kirschstein National Research Service Award (NRSA) Individual Postdoctoral Fellowship F32 5F32GM131570 (M.C.); National Science Foundation (NSF) Enabling Discovery through GEnomics (EDGE) grant 2128267, and the Center for Evolutionary Science at California Institute of Technology.

Conflicts of interest

The authors declare that there is no conflict of interest.

Literature cited

Barrière A, Félix M-A. 2006. Isolation of *C. elegans* and related nematodes. In Wormbook, The *C. elegans* Research Community. p. 1–9. doi/10.1895/wormbook.1.115.1, http://www.wormbook.org

Bhat AH, Chaubey AK, Shokoohi E, Mashela PW. 2019. Study of *Steinernema hermaphroditum* (Nematoda, Rhabditida), from the West Uttar Pradesh, India. Acta Parasitol. 64:720–737.

Bird AF, Akhurst RJ. 1983. The nature of the intestinal vesicle in nematodes of the family steinernematidae. Int J Parasitol. 13:599–606.

Bobardt SD, Dillman AR, Nair MG. 2020. The two faces of nematode infection: virulence and immunomodulatory molecules from nematode parasites of mammals, insects and plants. Front Microbiol. 11:577846.

Boemare NE, Akurst RJ. 1988. Biochemical and physiological characterization of colony form variants in *Xenorhabdus* spp. (Enterobacteriaceae). J Gen Microbiol. 134:751–761.

Bolt BJ, Rodgers FH, Shafie M, Kersey PJ, Berriman M, *et al.* 2018. Eukaryotic genomic databases, methods and protocols. Methods Mol Biology. 1757:471–491.

Bosch TCG, Guillemin K, McFall-Ngai M. 2019. Evolutionary "experiments" in symbiosis: the study of model animals provides insights into the mechanisms underlying the diversity of host–-microbe interactions. Bioessays. 41:1800256.

Boyer HW, Roulland-Dussoix D. 1969. A complementation analysis of the restriction and modification of DNA in *Escherichia coli*. J Mol Biol. 41:459–472.

Brenner S. 1974. The genetics of *Caenorhabditis elegans*. Genetics. 77: 71–94.

Cao M, Patel T, Rickman T, Goodrich-Blair H, Hussa EA. 2017. High levels of the *Xenorhabdus nematophila* transcription factor Lrp promote mutualism with the *Steinernema carpocapsae* nematode host. Appl Environ Microb. 83:e00276-17.

Chang DZ, Serra L, Lu D, Mortazavi A, Dillman AR. 2019. A core set of venom proteins is released by entomopathogenic nematodes in the genus *Steinernema*. Plos Pathog. 15:e1007626.

Chaston JM, Murfin KE, Heath-Heckman EA, Goodrich-Blair H. 2013. Previously unrecognized stages of species-specific colonization in the mutualism between *Xenorhabdus* bacteria and *Steinernema* nematodes: species-specific host colonization by *Xenorhabdus*. Cell Microbiol. 15:1545–1559.

Ciche TA, Ensign JC. 2003. For the insect pathogen *Photorhabdus luminescens*, which end of a nematode is out? Appl Environ Microbiol. 69:1890–1897.

Ciche TA, Sternberg PW. 2007. Postembryonic RNAi in *Heterorhabditis bacteriophora*: a nematode insect parasite and host for insect pathogenic symbionts. BMC Dev Biol. 7:101.

Cohen-Nissan SZ, Glazer I, Segal D. 1992. Phenotypic and genetic analysis of a mutant of *Heterorhabditis bacteriophora* Strain HP88. J Nematol. 24:359–364.

Curran J. 1989. Chromosome numbers of *Steinernema* and *Heterorhabditis* species. Rev Nematol. 12:145–148.

Dejima K, Hori S, Iwata S, Suehiro Y, Yoshina S, *et al.* 2018. An aneuploidy-free and structurally defined balancer chromosome toolkit for *Caenorhabditis elegans*. Cell Rep. 22:232–241.

Dillman AR, Guillermin ML, Lee JH, Kim B, Sternberg PW, *et al.* 2012. Olfaction shapes host-parasite interactions in parasitic nematodes. Proc Natl Acad Sci U S A. 109:e2324–e2333.

Dillman AR, Macchietto M, Porter CF, Rogers A, Williams B, *et al.* 2015. Comparative genomics of *Steinernema* reveals deeply conserved gene regulatory networks. Genome Biol. 16:200.

Dix I, Burnell AM, Griffin CT, Joyce SA, Nugent MJ, *et al.* 1992. The identification of biological species in the genus *Heterorhabditis*. (Nematoda: Heterorhabditidae) by cross-breeding second-generation amphimictic adults. Parasitology. 104:509–518.

Dolgin ES, Charlesworth B, Baird SE, Cutter AD. 2007. Inbreeding and outbreeding depression in *Caenorhabditis* nematodes. Evolution. 61:1339–1352.

Dunphy G, Webster JM. 1989. Monoxenic culture of *Neoaplectana carpocapsae* DD 136 and *Heterorhabditis*. Rev Nematol. 2:113–123.

Ehlers R-U. 2001. Mass production of entomopathogenic nematodes for plant protection. Appl Microbiol Biotechnol. 56:623–633.

Fire AZ. 2007. Gene silencing by double-stranded RNA (Nobel Lecture). Angew Chem Int Ed Engl. 46:6966–6984.

Flores-Lara Y, Renneckar D, Forst S, Goodrich-Blair H, Stock P. 2007. Influence of nematode age and culture conditions on morphological and physiological parameters in the bacterial vesicle of *Steinernema carpocapsae* (Nematoda: Steinernematidae). J Invertebr Pathol. 95:110–118.

Forst S, Clarke D. 2002. Entomopathogenic nematology. In R Gaugler, editor. Entomopathogenic Nematology. Wallingford: CABI. p. 57–77.

Forst S, Dowds B, Boemare N, Stackebrandt E. 1997. *Xenorhabdus* and *Photorhabdus* spp.: bugs that kill bugs. Annu Rev Microbiol. 51: 47–72.

Frézal L, Félix M-A. 2015. *C. elegans* outside the Petri dish. Elife. 4: e05849.

Gang SS, Castelletto ML, Bryant AS, Yang E, Mancuso N, *et al.* 2017. Targeted mutagenesis in a human-parasitic nematode. Plos Pathog. 13:e1006675.

Gang SS, Castelletto ML, Yang E, Ruiz F, Brown TM, *et al.* 2020. Chemosensory mechanisms of host seeking and infectivity in skin-penetrating nematodes. Proc Natl Acad Sci U S A. 117: 17913–17923.

Gang SS, Hallem EA. 2016. Mechanisms of host seeking by parasitic nematodes. Mol Biochem Parasitol. 208:23–32.

Goodrich-Blair H, Clarke DJ. 2007. Mutualism and pathogenesis in *Xenorhabdus* and *Photorhabdus*: two roads to the same destination: bacteria-host interactions. Mol Microbiol. 64:260–268.

Griffin CT, O'Callaghan KM, Dix I. 2001. A self-fertile species of *Steinernema* from Indonesia: further evidence of convergent evolution amongst entomopathogenic nematodes? Parasitology. 122:181–186.

Hallem EA, Dillman AR, Hong AV, Zhang Y, Yano JM, *et al.* 2011. A sensory code for host seeking in parasitic nematodes. Curr Biol. 21:377–383.

Hashmi S, Hashmi G, Gaugler R. 1995. Genetic transformation of an entomopathogenic nematode by microinjection. J Invertebr Pathol. 66:293–296.

Heger P, Kroiher M, Ndifon N, Schierenberg E. 2010. Conservation of MAP kinase activity and MSP genes in parthenogenetic nematodes. BMC Dev Biol. 10:51.

Herbert EE, Goodrich-Blair H. 2007. Friend and foe: the two faces of *Xenorhabdus nematophila*. Nat Rev Microbiol. 5:634–646.

Hopper KR, Roush RT, Powell W. 2003. Management of genetics of biological-control introductions. Annu Rev Entomol. 38:27–51.

Horvitz HR. 2003. Nobel lecture: worms, life and death. Bioscience Rep. 23:239–303.

Kim DH, Flavell SW. 2020. Host-microbe interactions and the behavior of *Caenorhabditis elegans*. J Neurogenet. 34:1–10.

Kim SK, Flores-Lara Y, Stock SP. 2012. Morphology and ultrastructure of the bacterial receptacle in *Steinernema* nematodes (Nematoda: Steinernematidae). J Invertebr Pathol. 110: 366–374.

Kocsisova Z, Kornfeld K, Schedl T. 2019. Rapid population-wide declines in stem cell number and activity during reproductive aging in *C. elegans*. Development. 146:dev173195.

Kocsisova Z, Mohammad A, Kornfeld K, Schedl T. 2018. Cell cycle analysis in the *C. elegans* germline with the thymidine analog EdU. J Vis Exp 58339. doi:10.3791/58339.

Kosinski M, McDonald K, Schwartz J, Yamamoto I, Greenstein D. 2005. C. elegans sperm bud vesicles to deliver a meiotic maturation signal to distant oocytes. Development. 132:3357–3369. 10.1242/dev.01916 15975936

Kroetz SM, Srinivasan J, Yaghoobian J, Sternberg PW, Hong RL. 2012. The cGMP signaling pathway affects feeding behavior in the necromenic nematode *Pristionchus pacificus*. PLoS One. 7:e34464.

LaMunyon CW, Ward S. 1998. Larger sperm outcompete smaller sperm in the nematode *Caenorhabditis elegans*. Proc Biol Sci. 265: 1997–2002.

Lightfoot JW, Wilecki M, Rödelsperger C, Moreno E, Susoy V, *et al.* 2019. Small peptide–mediated self-recognition prevents cannibalism in predatory nematodes. Science. 364:86–89.

Link CD, Graf-Whitsel J, Wood WB. 1987. Isolation and characterization of a nematode transposable element from *Panagrellus redivivus*. Proc Natl Acad Sci U S A. 84:5325–5329.

Liu C, De SL, Miley K, Unnasch TR. 2020. In vivo imaging of transgenic *Brugia malayi*. Plos Negl Trop Dis. 14:e0008182.

Lok JB. 2019. CRISPR/Cas9 mutagenesis and expression of dominant mutant transgenes as functional genomic approaches in parasitic nematodes. Front Genet. 10: 656. doi: 10.3389/fgene.2019.00656.

Martens EC, Goodrich-Blair H. 2005. The *Steinernema carpocapsae* intestinal vesicle contains a subcellular structure with which *Xenorhabdus nematophila* associates during colonization initiation. Cell Microbiol. 7:1723–1735.

McFall-Ngai M, Hadfield MG, Bosch TCG, Carey HV, Domazet-Lošo T, *et al.* 2013. Animals in a bacterial world, a new imperative for the life sciences. Proc Natl Acad Sci U S A. 110:3229–3236.

Mello CC. 2007. Return to the RNAi world: rethinking gene expression and evolution (Nobel Lecture). Angew Chem Int Ed Engl. 46: 6985–6994.

Miller MA, Nguyen VQ, Lee M-H, Kosinski M, Schedl T, *et al.* 2001. A sperm cytoskeletal protein that signals oocyte meiotic maturation and ovulation. Science. 291:2144–2147.

Moerman DG, Baillie DL. 1979. Genetic organization in *Caenorhabditis elegans*: fine-structure analysis of the *unc-22* gene. Genetics. 91: 95–103.

Morais LH, Schreiber HL, Mazmanian SK. 2021. The gut microbiota–-brain axis in behaviour and brain disorders. Nat Rev Microbiol. 19:241–255.

Murfin KE, Chaston J, Goodrich-Blair H. 2012. Visualizing bacteria in nematodes using fluorescent microscopy. J Vis Exp.4298. doi: 10.3791/4298.

NCBI Resource Coordinators. 2017. Database resources of the National Center for Biotechnology Information. Nucleic Acids Res. 45:D12–D17.

Nigon VM, Félix M-A. 2017. History of research on *C. elegans* and other free-living nematodes as model organisms. In: Wormbook, editor. The C. elegans Research Community. Vol. 2017. p. 1–84. doi/10.1895/wormbook.1.181.1, http://www.wormbook.org

O'Connell KF. 2021. Cryopreservation of *C. elegans* and other nematodes with Dimethyl Sulfoxide and Trehalose. In: G Haspel, AC Hart, editors. C. elegans Methods and Applications, 3rd ed. New York: Springer/Nature.

Park Y, Herbert EE, Cowles CE, Cowles KN, Menard ML, *et al.* 2007. Clonal variation in *Xenorhabdus nematophila* virulence and suppression of *Manduca sexta* immunity. Cell Microbiol. 9:645–656.

Popiel I, Vasquez E. 1991. Cryopreservation of *Steinernema carpocapsae* and *Heterorhabditis bacteriophora*. J Nematol. 23:432–437.

Rahimi FR, McGuire TR, Gaugler R. 1993. Morphological mutant in the entomopathogenic nematode, *Heterorhabditis bacteriophora*. J Hered. 84:475–478.

Ratnappan R, Vadnal J, Keaney M, Eleftherianos I, O'Halloran D, *et al.* 2016. RNAi-mediated gene knockdown by microinjection in the model entomopathogenic nematode *Heterorhabditis bacteriophora*. Parasit Vectors. 9:160.

Roberts TM, Stewart M. 1995. Nematode sperm locomotion. Curr Opin Cell Biol. 7:13–17.

Roh HC, Collier S, Guthrie J, Robertson JD, Kornfeld K. 2012. Lysosome-related organelles in intestinal cells are a zinc storage site in *C. elegans*. Cell Metab. 15:88–99.

Rougon-Cardoso A, Flores-Ponce M, Ramos-Aboites HE, Martínez-Guerrero CE, Hao Y-J, *et al.* 2016. The genome, transcriptome, and proteome of the nematode *Steinernema carpocapsae*: evolutionary signatures of a pathogenic lifestyle. Sci Rep. 6:37536.

Ruby EG. 2008. Symbiotic conversations are revealed under genetic interrogation. Nat Rev Microbiol. 6:752–762.

Schiffer PH, Polsky AL, Cole AG, Camps JIR, Kroiher M, *et al.* 2018. The gene regulatory program of *Acrobeloides nanus* reveals conservation of phylum-specific expression. Proc National Acad Sci U S A. 115:201720817.

Serra L, Macchietto M, Macias-Munoz A, McGill CJ, Rodriguez IM, *et al.* 2019. Hybrid assembly of the genome of the entomopathogenic nematode *Steinernema carpocapsae* identifies the X-chromosome. G3 (Bethesda). 9:2687–2697.

Shapira M. 2017. Host–microbiota interactions in *Caenorhabditis elegans* and their significance. Curr Opin Microbiol. 38:142–147.

Shinya R, Hasegawa K, Chen A, Kanzaki N, Sternberg PW. 2014. Evidence of hermaphroditism and sex ratio distortion in the fungal feeding nematode *Bursaphelenchus okinawaensis*. G3. 4:1907–1917.

Shtonda BB, Avery L. 2006. Dietary choice behavior in *Caenorhabditis elegans*. J Exp Biol. 209:89–102.

Snyder H, Stock SP, Kim S-K, Flores-Lara Y, Forst S. 2007. New insights into the colonization and release processes of *Xenorhabdus nematophila* and the morphology and ultrastructure of the bacterial receptacle of its nematode host, *Steinernema carpocapsae*. Appl Environ Microbiol. 73:5338–5346.

Sommer R. 2006. *Pristionchus pacificus*. In: Wormbook, editor. The C. elegans Research Community, WormBook, p. 1–8. doi/10.1895/-wormbook.1.102.1, http://www.wormbook.org.

Stiernagle T. 2006. Maintenance of *C. elegans*. In Wormbook editor. The C. elegans Research Community, WormBook, p. 1–11. doi/10.1895/wormbook.1.101.1, http://www.wormbook.org.

Stock P, Griffin CT, Chaerani R. 2004. Morphological and molecular characterisation of *Steinernema hermaphroditum n. sp*. (Nematoda: Steinernematidae), an entomopathogenic nematode from Indonesia, and its phylogenetic relationships with other members of the genus. Nematology. 6:401–412.

Sugar DR, Murfin KE, Chaston JM, Andersen AW, Richards GR, *et al.* 2011. Phenotypic variation and host interactions of *Xenorhabdus bovienii* SS-2004, the entomopathogenic symbiont of *Steinernema jollieti* nematodes. Environ Microbiol. 14:924–939.

Sulston JE, Horvitz HR. 1977. Post-embryonic cell lineages of the nematode, *Caenorhabditis elegans*. Dev Biol. 56:110–156.

Surrey MR, Davies RJ. 1996. Pilot-scale liquid culture and harvesting of an entomopathogenic nematode, *Heterorhabditis bacteriophora*. J Invertebr Pathol. 67:92–99.

Tailliez P, Pagès S, Ginibre N, Boemare N. 2006. New insight into diversity in the genus *Xenorhabdus*, including the description of ten novel species. Int J Syst Evol Microbiol. 56:2805–2818.

Tarasco E, Ragni A, Curto G. 2017. Biocontrol Agents: Entomopathogenic and Slug Parasitic Nematodes. p. 429–444.

Vielle A, Callemeyn-Torre N, Gimond C, Poullet N, Gray JC, *et al.* 2016. Convergent evolution of sperm gigantism and the developmental origins of sperm size variability in *Caenorhabditis nematodes*. Evolution. 70:2485–2503.

Vivas EI, Goodrich-Blair H. 2001. *Xenorhabdus nematophilus* as a model for host-bacterium interactions: *rpoS* is necessary for mutualism with nematodes. J Bacteriol. 183:4687–4693.

Volgyi A, Fodor A, Szentirmai A, Forst S. 1998. Phase variation in *Xenorhabdus nematophilus*. Appl Environ Microbiol. 64:1188–1193.

Ward S, Carrel JS. 1979. Fertilization and sperm competition in the nematode *Caenorhabditis elegans*. Dev Biol. 73:304–321.

Watson E, MacNeil LT, Ritter AD, Yilmaz LS, Rosebrock AP, *et al.* 2014. Interspecies systems biology uncovers metabolites affecting *C. elegans* gene expression and life history traits. Cell. 156: 759–770.

White GF. 1927. A method for obtaining infective nematode larvae from cultures. Science. 66:302–303.

Winter ES, Schwarz A, Fabig G, Feldman JL, Pires-daSilva A, *et al.* 2017. Cytoskeletal variations in an asymmetric cell division support diversity in nematode sperm size and sex ratios. Development. 144:3253–3263.

Xu J, Hurlbert RE. 1990. Toxicity of irradiated media *for Xenorhabdus spp*. Appl Environ Microbiol. 56:815–818.

Zhang F, Weckhorst JL, Assié A, Hosea C, Ayoub CA, *et al.* 2021. Natural genetic variation drives microbiome selection in the *Caenorhabditis elegans* gut. Curr Biol. 31:2603–2618.e9.

Communicating editor: B. Conradt